

### Electronic Supplementary Information

#### **Reduced Graphene Oxide Integrated Poly(ionic liquid) Functionalized Nano-fibrillated Cellulose Composite Paper with Improved Toughness, Ductility and Hydrophobicity**

Rama K. Layek<sup>a,b,\*</sup>, Vijay Singh Parihar<sup>c</sup>, Jukka Seppälä<sup>d</sup>, Alexander Efimov<sup>e</sup>, Sarianna Palola<sup>a</sup>, Mikko Kanerva<sup>a</sup>, Shambhavee Annurakshita<sup>f</sup>, Minna Kellomäki<sup>c</sup>, Essi Sarlin<sup>a</sup>

<sup>a</sup>Tampere University, Engineering Material Science, P.O. Box 589, 33101 Tampere, Finland

<sup>b</sup>Department of Separation Science, School of Engineering Science, LUT University, Mikkulankatu 19, 15210 Lahti, Finland

<sup>c</sup>Biomaterials and Tissue Engineering Group, BioMediTech, Faculty of Medicine and Health Technology, Tampere University

<sup>d</sup>Polymer Technology, School of Chemical Engineering, Aalto University, Finland

<sup>e</sup>Faculty of Engineering and Natural Science, Tampere University

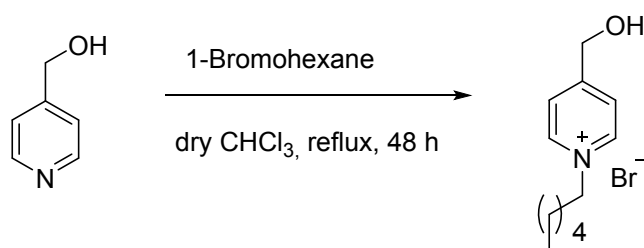
<sup>f</sup>Photonics Laboratory, Tampere University, 33720 Tampere, Finland

---

\*Corresponding author. Tel: +35850 4478355. E-mail : [rama.layek@tuni.fi](mailto:rama.layek@tuni.fi) (Rama Kanta Layek).

## Experimental Section

### Synthesis of 1-hexyl-4-(hydroxymethyl) pyridinium bromide (Pyridinium II):

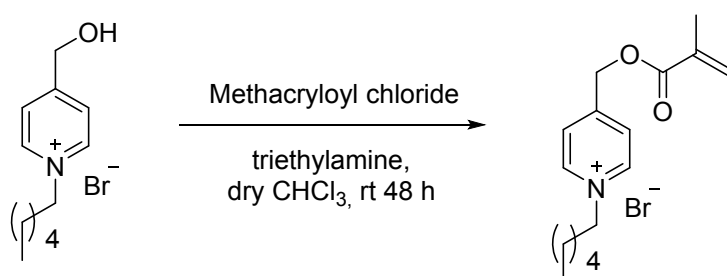


5.0 g of 4-pyridinemethanol was dissolved in 50 mL dry chloroform taken in seal tube and 2 equivalents of 1-bromohexane was added to it and then refluxed for 48 h. Then the reaction was brought to room temperature and the solvent was evaporated. The crude product was washed with dry hexane and followed by dry ethyl acetate. The traces of the solvent were removed by using a high vacuum pump to afford 1-alkyl-4-(hydroxymethyl) pyridinium bromides in 80 to 85 % yield.

$^1\text{H-NMR}$  (500 MHz,  $\text{D}_2\text{O}$ )  $\delta/\text{ppm}$ : 8.80-8.84 (dd, 2H), 8.04-8.01 (dd, 2H), 4.98 (s, 2H), 4.63-4.54 (m, 2H), 2.03-1.98 (m, 2H), 1.32-1.11 (m, 6H), 0.82-0.79 (t, 3H).

$^{13}\text{C-NMR}$  (125 MHz,  $\text{D}_2\text{O}$ )  $\delta/\text{ppm}$ : 161.69 (qt-C-Ar), 143.86 ( -CH=N<sup>+</sup>- Ar), 124.81 (-CH=, Ar), 61.7 (-CH<sub>2</sub>-OH), 61.42 (N<sup>+</sup>-CH<sub>2</sub>-), 30.65 (N<sup>+</sup>-CH<sub>2</sub>-CH<sub>2</sub>-), 30.48 (N<sup>+</sup>-CH<sub>2</sub>-CH<sub>2</sub>-CH<sub>2</sub>-), 25.03 (-CH<sub>2</sub>-CH<sub>2</sub>-CH<sub>3</sub>), 21.90 (-CH<sub>2</sub>-CH<sub>3</sub>), 13.48 (-CH<sub>3</sub>).

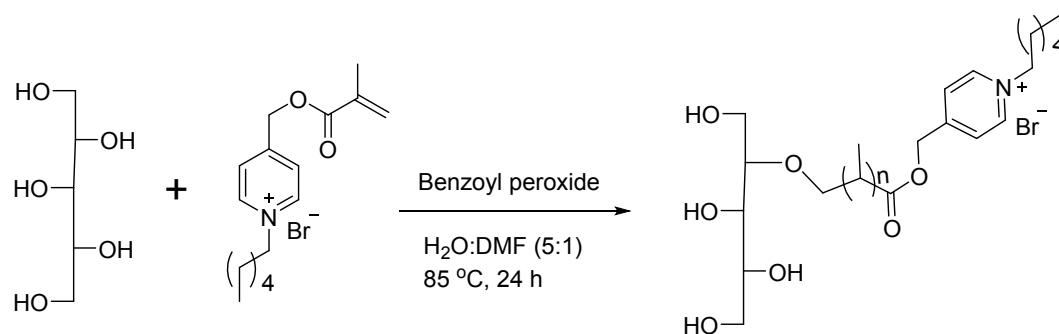
### Synthesis of 1-hexyl-4-(methacryloyloxy-methyl) pyridinium bromide (Pyridinium II acrylate):



3.0 g of alkylated pyridine derivative was dissolved in 50 mL of dry chloroform in 100 mL round bottom flask and then triethylamine (catalytic 0.2 mL) was added to the solution. After cooling the solution to about 0 °C, 2 mL (around 1.6 equivalent) of methacryloyl chloride was added dropwise. The reaction mixture was stirred at room temperature for 48 h and reaction progression monitored by TLC. After the completion of the reaction, the reaction mixture was dried over the rotary evaporator and extracted with water and chloroform. The organic layer

was dried over  $\text{MgSO}_4$  and solvent was evaporated which afford crude product with 73% yield. The compound was purified by column chromatography (Dichloromethane:Methanol, 93:07).  $^1\text{H-NMR}$  (500 MHz,  $\text{CDCl}_3$ )  $\delta/\text{ppm}$ : 9.48-9.46 (dd, 2H), 8.04-8.02 (dd, 2H), 6.18 (d, 1H,  $\text{C}=\text{CH}_2$ ), 5.66 (d, 1H,  $\text{C}=\text{CH}_2$ ), 5.42 (s, 2H), 4.90-4.85 (m, 2H), 2.00-1.85 (m, 5H,  $\text{N}^+\text{-CH}_2$ ,  $\text{CH}_3\text{-C=}$ ), 1.31-1.18 (m, 6H), 0.77-0.74 (t, 3H).  $^{13}\text{C-NMR}$  (125 MHz,  $\text{CDCl}_3$ )  $\delta/\text{ppm}$ : 166.28 ( $\text{C}=\text{O}$ ), 156.14 (qt-C-Ar), 145.16 ( $-\text{CH}=\text{N}^+\text{-Ar}$ ), 134.95 ( $\text{C}=\text{C}$ ), 127.89 ( $\text{C}=\text{C}$ ), 124.81 ( $-\text{CH}=\text{Ar}$ ), 63.44 ( $-\text{CH}_2\text{-OH}$ ), 61.58 ( $\text{N}^+\text{-CH}_2\text{-}$ ), 31.91 ( $\text{N}^+\text{-CH}_2\text{-CH}_2\text{-}$ ), 31.14 ( $\text{N}^+\text{-CH}_2\text{-CH}_2\text{-CH}_2\text{-}$ ), 25.69 ( $-\text{CH}_2\text{-CH}_2\text{-CH}_3$ ), 22.37 ( $-\text{CH}_2\text{-CH}_3$ ), 18.33 ( $\text{CH}_3\text{-C}=\text{C}-$ ), 13.98 ( $-\text{CH}_3$ ).

### Grafting of IL-acrylate (1-hexyl-4-(methacryloyloxy-methyl) pyridinium bromide) on nanofibrillated cellulose (NFC-g-PIL)



NFC (1 g neat) was dispersed in 100 mL deionized water and sonicated for 5 minutes. Ionic liquid methacrylate (1.5 g) was dissolved in 20 mL of DMF and added to the reaction mixture and purged with nitrogen for 30 minutes. Benzoyl peroxide (150 mg) was dissolved in 5 mL of DMF and added to the reaction mixture in a nitrogen atmosphere and stirred at  $85\text{ }^\circ\text{C}$  for 24 hours. The reaction mixture was cooled to room temperature and filtered by using nylon filter paper and washed with DMF and deionized water several times to remove the unreacted monomers and free polymer, if any.

### Fabrication of NFC, NFC-g-PIL, rGO1/NFC and rGO1/NFC-g-PIL composite films:

The NFC was purchased (Solids: 15.0%, Grade: 90%, Sample description: Cake) from Process Development Center of the University of Maine, USA that was prepared by mechanical treatment of bleached softwood kraft pulp. To fabricate free-standing NFC and NFC-g-PIL film, 500 mL aqueous dispersion of (1.4 mg/mL) NFC and NFC-g-PIL solutions were prepared

by ultrasonication for 30 min. Then, these aqueous dispersions of NFC and NFC-g-PIL were filtered under vacuum through a cellulose acetate membrane. Finally, NFC and NFC-g-PIL composite papers were obtained by drying at room temperature followed by pressing at 70 °C for 2 minutes.

To fabricate free-standing rGO1/NFC and rGO1/NFC-g-PIL films, rGO solution was prepared by reducing the GO in 9:1 DMF:H<sub>2</sub>O solution by hydrazine hydrated treatment followed by ultrasonication. Then, the aqueous dispersion of rGO1/NFC and rGO1/NFC-g-PIL composite solution (where the number 1 represent 1 wt% of rGO w. r. t NFC and NFC-g-PIL) was prepared by mixing a required amount of rGO dispersion (in DMF:H<sub>2</sub>O = 9:1) with the necessary amount of aqueous solution of NFC and NFC-g-PIL. The final concentration of rGO1/NFC and rGO1/NFC-g-PIL dispersion was adjusted to 1.4 mg/mL and ultrasonicated for 30 min to obtain a homogeneous dispersion. Finally, the free-standing rGO1/NFC and rGO1/NFC-g-PIL composite films were fabricated by vacuum filtration of the aqueous dispersion of rGO1/NFC and rGO1/NFC-g-PIL solutions followed by drying at room temperature and pressing at 70 °C for 2 minutes.

### **Characterization**

All proton NMR were recorded using JEOL-500 MHz instrument (SCZ500R, JEOL Resonance, Japan). The Atomic force microscopy of rGO was carried out by casting a drop of 0.01%, (w/v) of rGO dispersion in DMF:H<sub>2</sub>O (9:1) on a mica surface followed by drying the drop of the solution through a noncontact mode by using a tip resonance frequency of 250 KHz. The AFM study of the NFC and NFC-g-PIL were performed by casting drop of a very dilute aqueous dispersion (0.01%, w/v) of NFC and NFC-g-PIL on a silicon wafer surface.

The samples for the field emission scanning electron microscopy study were prepared by freeze fracturing the samples in liquid nitrogen followed by sputtering of gold on the freeze-fracture surface. Then the fracture surfaces were observed by using a SEM Zeiss ULTRA Plus instrument. The FTIR spectroscopy of the rGO, NFC, rGO1/NFC, NFC-g-PIL and rGO1/NFC-g-PIL composite papers were recorded (Tensor 27 Bruker instrument) from 4000 – 400 cm<sup>-1</sup> in ATR mode. Thermogravimetry (TGA) study of the NFC and NFC-g-PIL composite films was performed in nitrogen environment from 40 °C to 600 °C with a heating rate of 10 °C/min using a Thermal Analyzer instrument (Netzsch STA 409). Water contact angles of the Nanocellulose based film were measured with the Attension Theta Lite optical tensiometer using a sessile drop method. A droplet of deionized water (3 μL) was slowly applied on the sample surface and simultaneously recorded using a video recorder for 10 seconds after the contact. Contact

angle (CA) values (left and right) were automatically calculated with the equipment software (OneAttention v2.1). The stress-strain study of the NFC, NFC-g-PIL, rGO1/NFC and rGO1/NFC-g-PIL composite papers (with a specimen size of 16 mm × 4 mm × 0.1 mm) were performed using an Instron 5967 instrument with a strain rate of 1 mm/min at room temperature by using a load cell of 500 N. NMR spectra were measured on 500 MHz JEOL LNM-ECZ500R spectrometer. The spectra were measured at room temperature. Liquid spectra were measured with a broadband inverse Royal HFX probe. Solid state MAS <sup>1</sup>H spectra were measured with the high-resolution field gradient FGMAS probe at 5 kHz spinning rate. Samples were packed in 3.2 mm zirconia spinners as a thick suspension in D<sub>2</sub>O. Solid state MAS <sup>13</sup>C spectra were recorded with the high-resolution cross-polarization HXMAS probe at 18 kHz spinning rate. Samples were packed in 3.2 mm zirconia spinners as dry materials.

Table 1. Contact angles of NFC, rGO1/NFC, NFC-g-PIL and rGO1/NFC-g-PIL paper

| Sample         | Contact angle |
|----------------|---------------|
| NFC            | 49±2°         |
| rGO1/NFC       | 66±1°         |
| NFC-g-PIL      | 65±1.5°       |
| rGO1/NFC-g-PIL | 75±1°         |

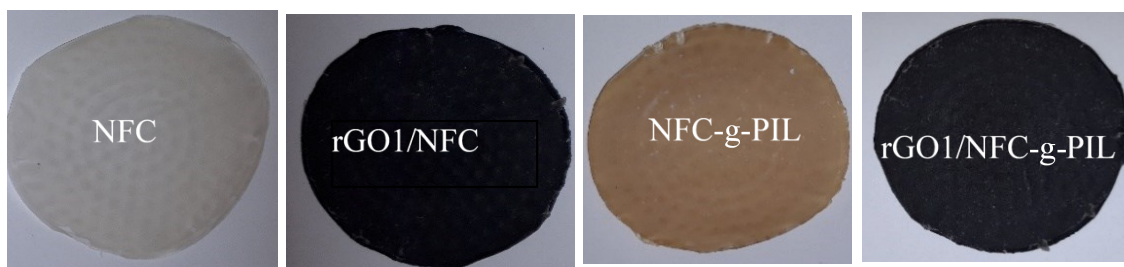


Figure 1. Digital photograph of NFC, rGO1/NFC, NFC-g-PIL and rGO1/NFC-g-PIL

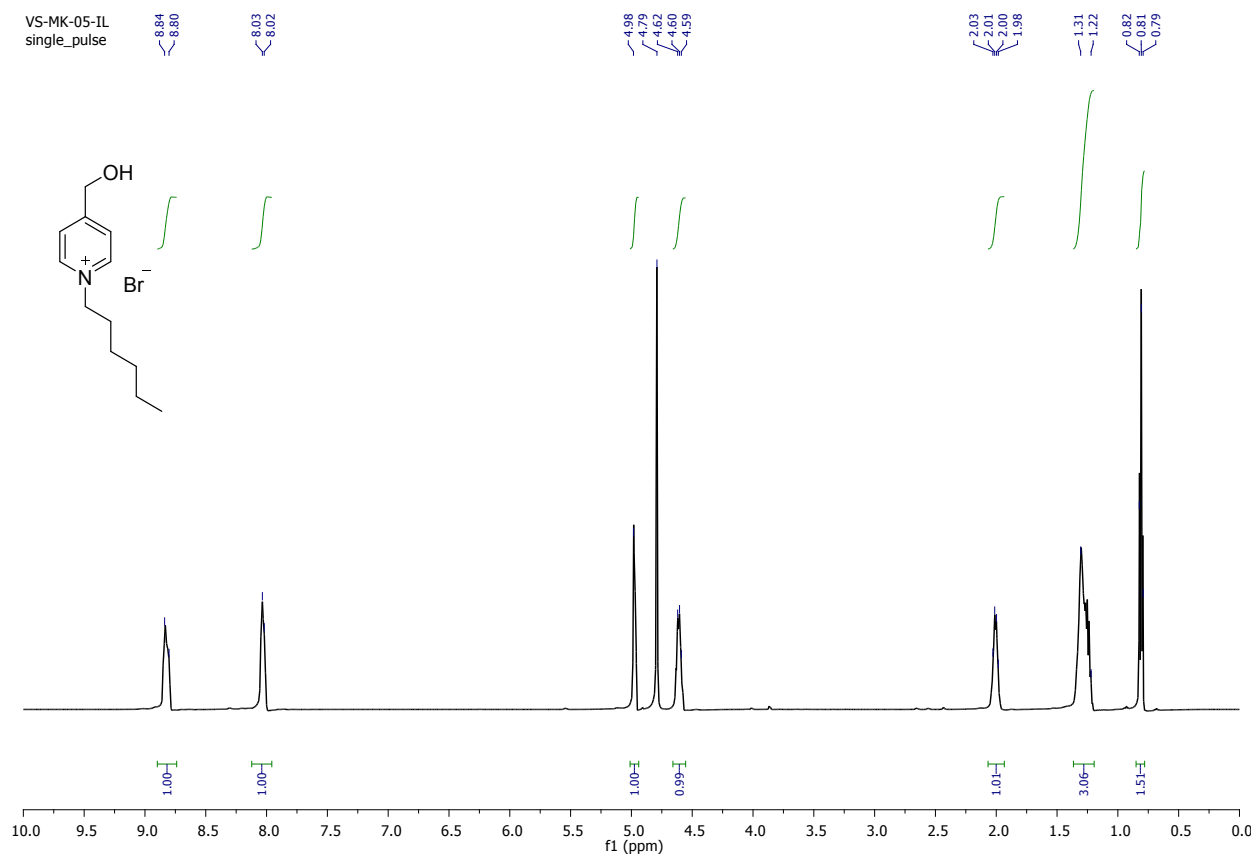


Figure 2.  $^1\text{H}$  NMR spectrum of pyridinium IL (500 MHz,  $\text{D}_2\text{O}$ )

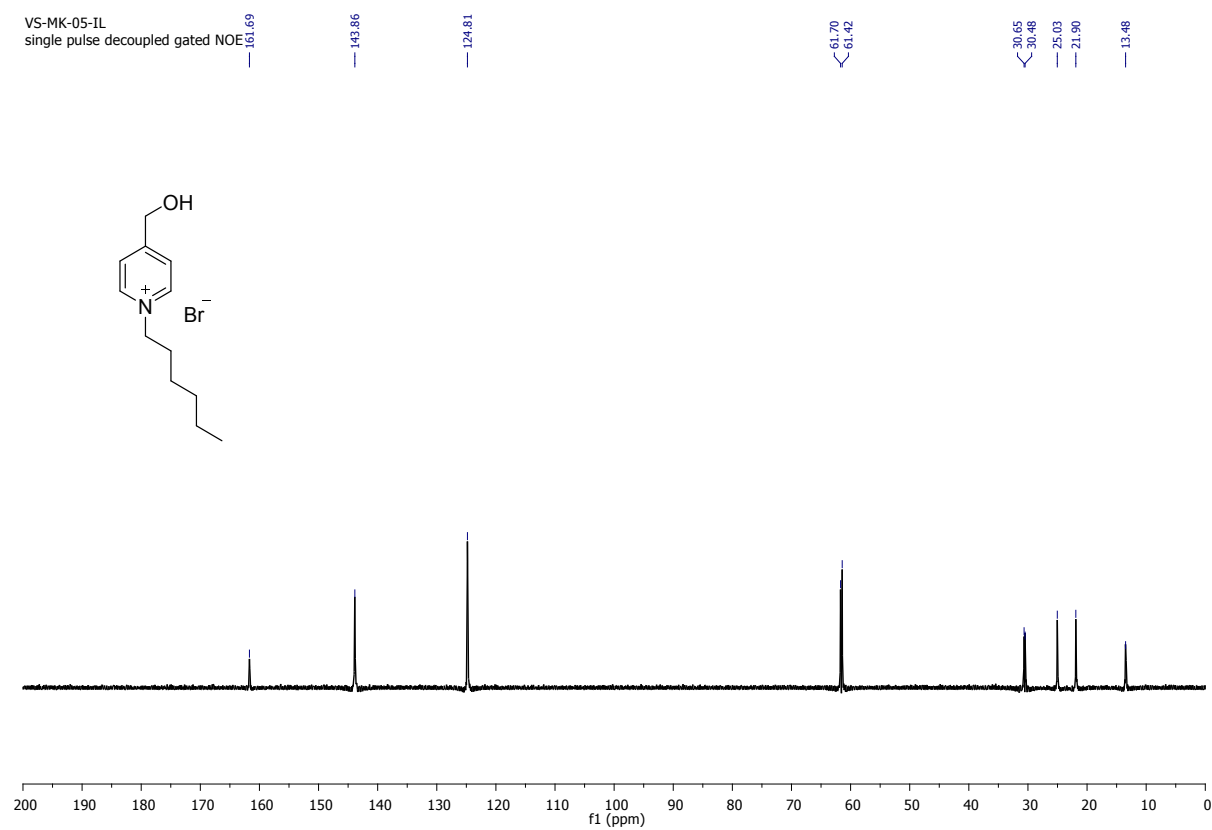


Figure 3.  $^{13}\text{C}$  NMR spectrum of pyridinium IL (125 MHz,  $\text{D}_2\text{O}$ )

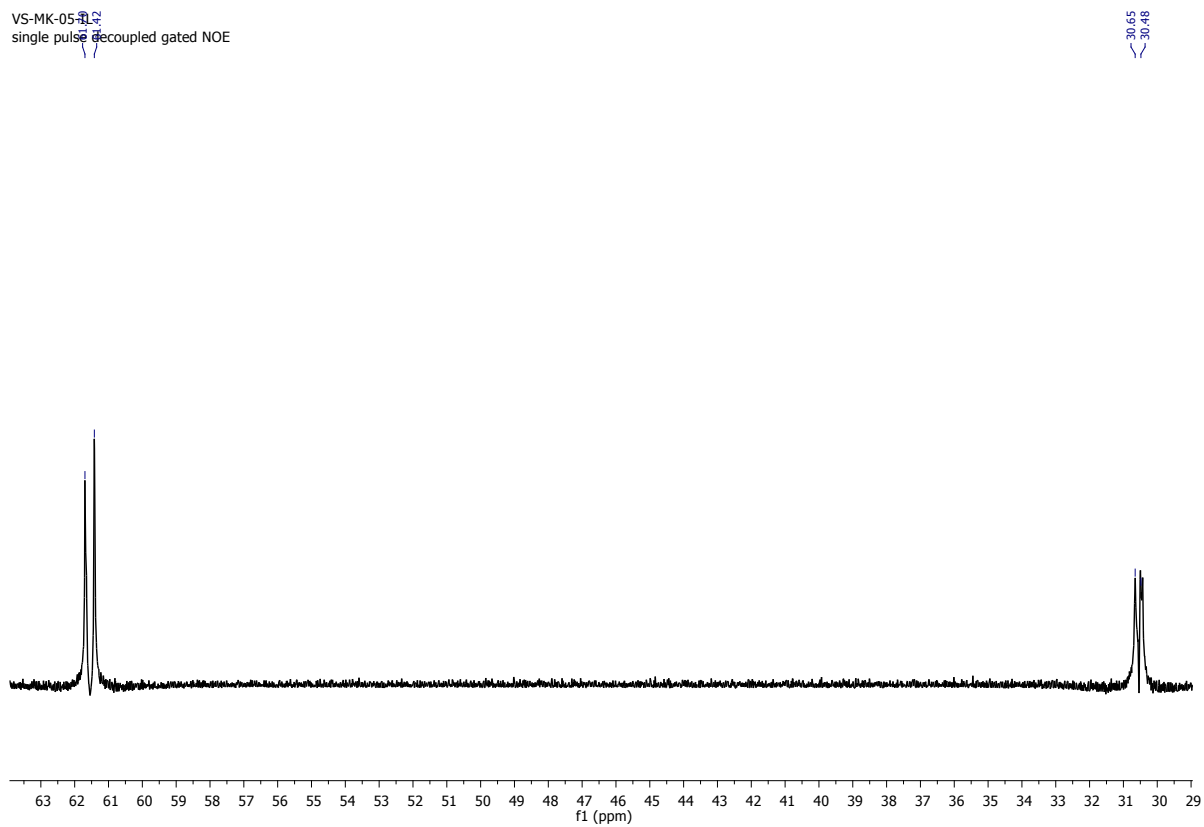


Figure 3(A). Enlarge  $^{13}\text{C}$  NMR spectrum of pyridinium IL (125 MHz,  $\text{D}_2\text{O}$ ) clearly showing the number of peaks.

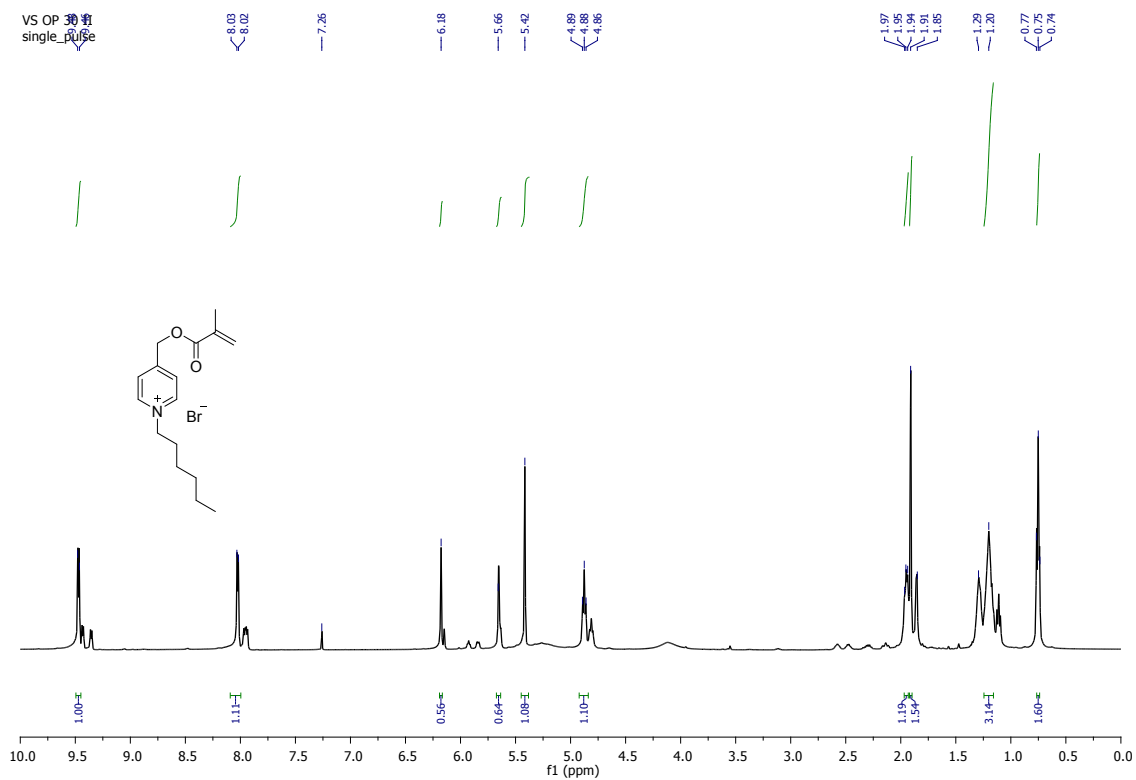


Figure 4.  $^1\text{H}$  NMR spectrum of pyridinium IL acrylate (500 MHz,  $\text{CDCl}_3$ )

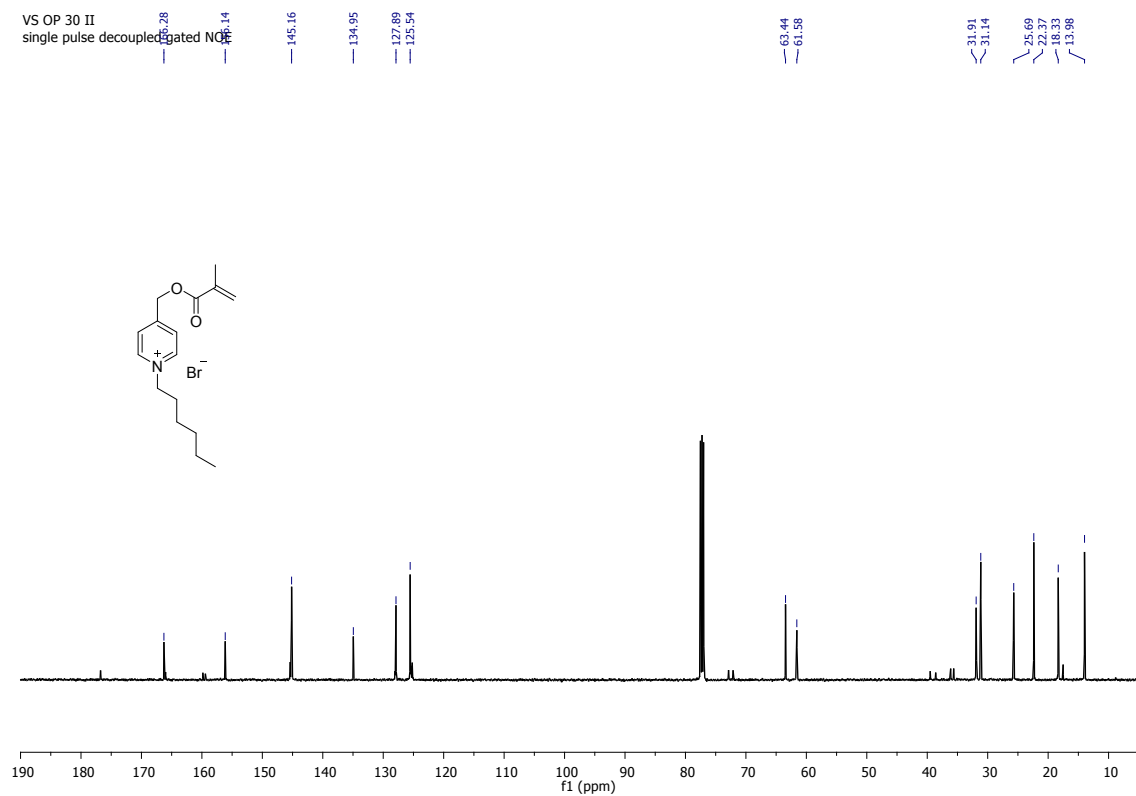


Figure 5.  $^{13}\text{C}$  NMR spectrum of pyridinium IL acrylate (125 MHz,  $\text{CDCl}_3$ )



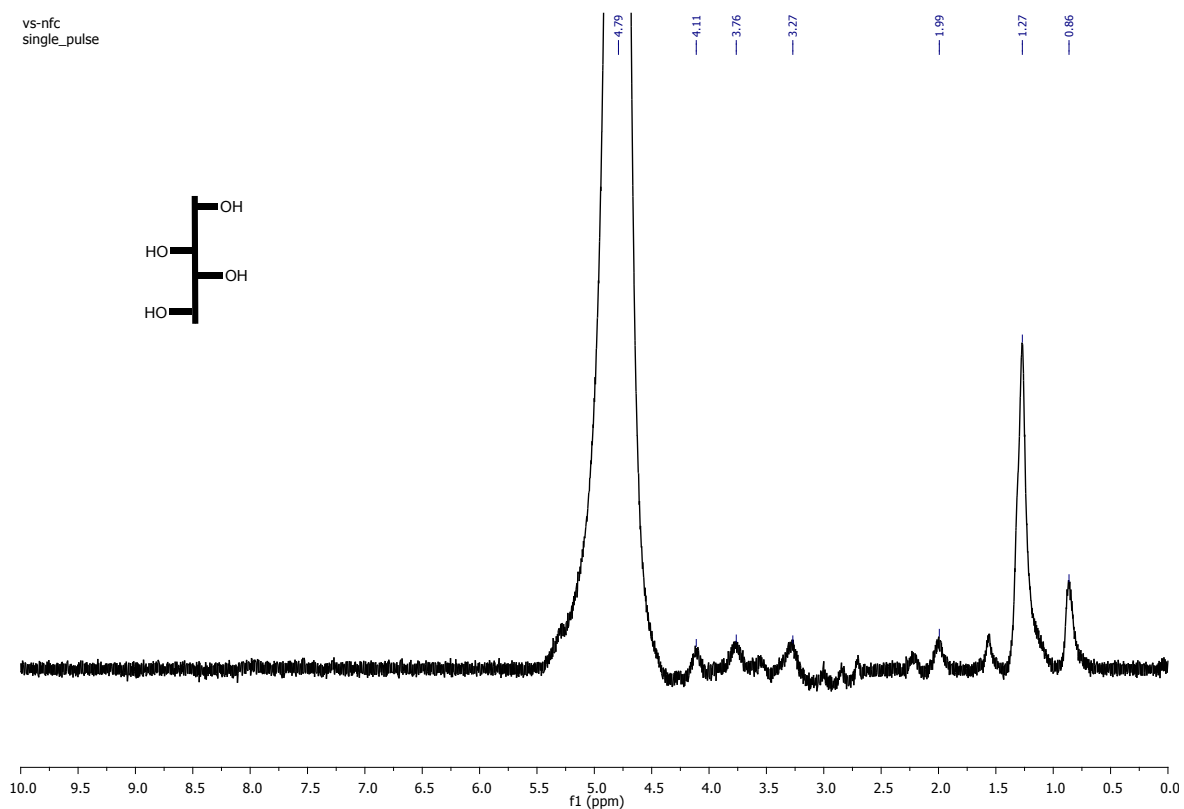


Figure 6. Solid state  $^1\text{H}$  NMR spectrum of pure NFC (500 MHz, small amount of  $\text{D}_2\text{O}$  for packing of the sample in sample holder, spinning 5 kHz)

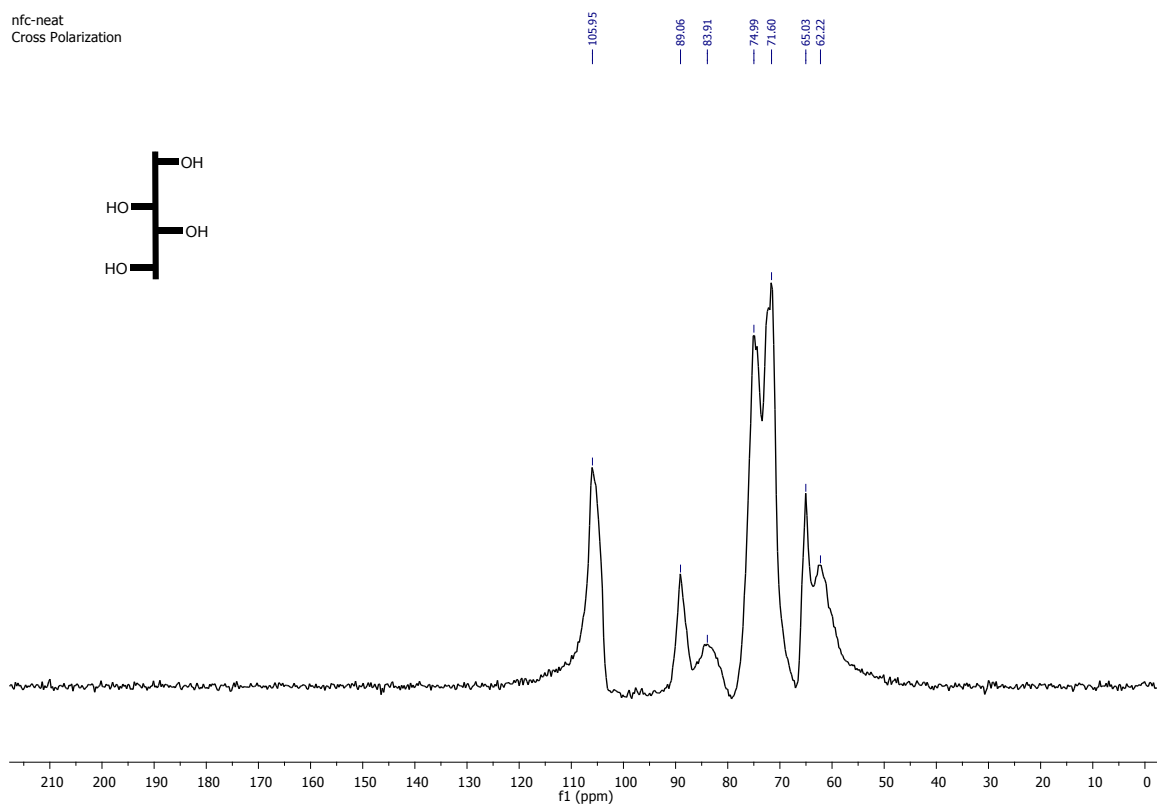


Figure 7. Solid-state Cross-Polarization Magic Angle Spinning  $^{13}\text{C}$  NMR spectrum of NFC (125 MHz, spinning 18 kHz )

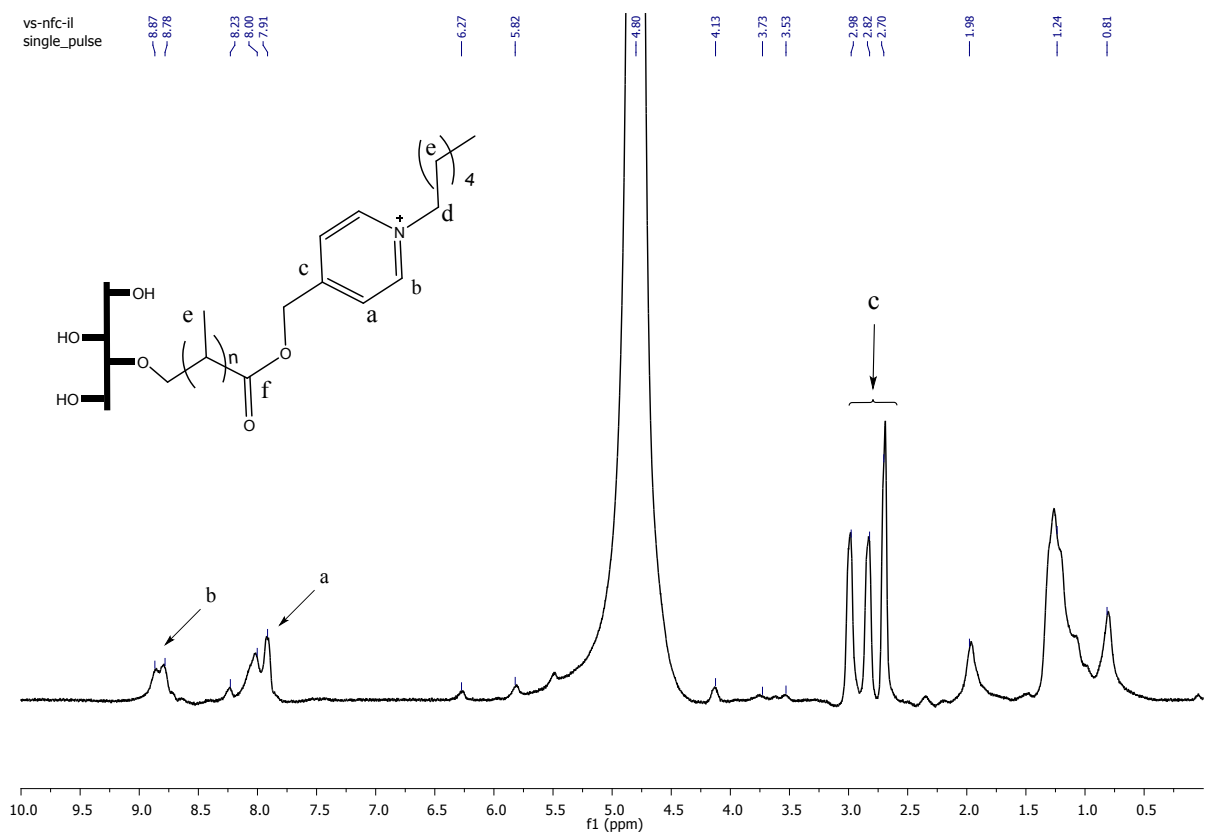


Figure 8. Solid state  $^1\text{H}$  NMR spectrum of pure NFC-g-PIL (500 MHz, small amount of  $\text{D}_2\text{O}$  for packing of the sample in sample holder, spinning 5 kHz)

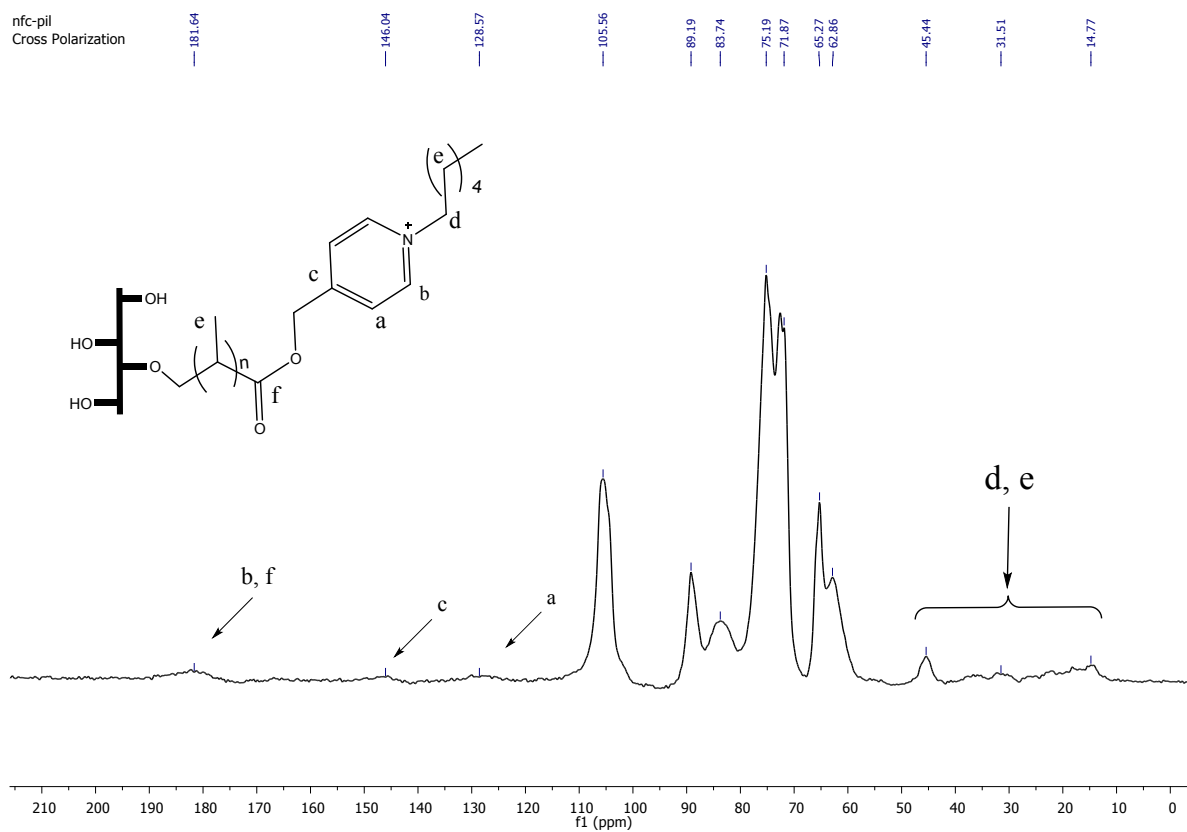


Figure 9 (A). Solid-state Cross-Polarization Magic Angle Spinning  $^{13}\text{C}$  NMR spectrum of NFC-g-PIL (125 MHz, spinning 18 kHz)

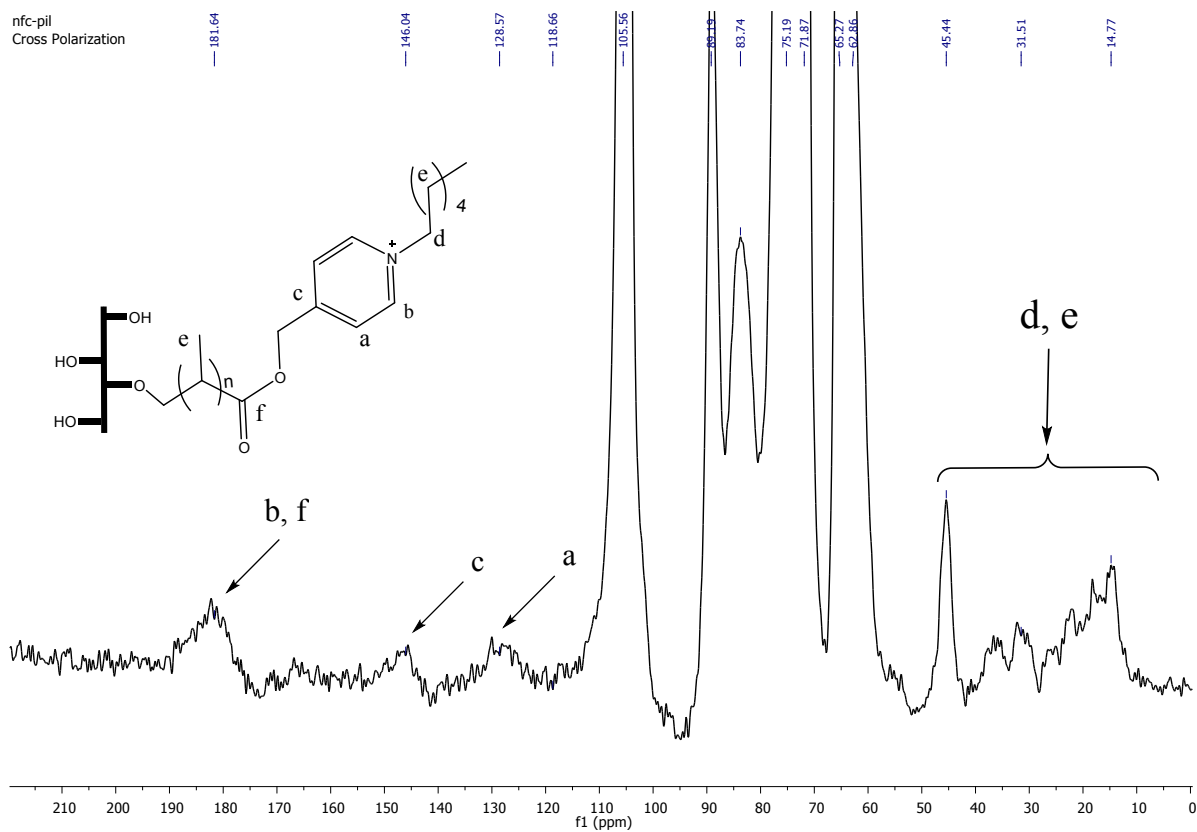


Figure 9 (B). Enlarge Solid-state Cross-Polarization Magic Angle Spinning <sup>13</sup>C NMR spectrum of NFC-g-PIL (125 MHz, spinning 18 kHz)

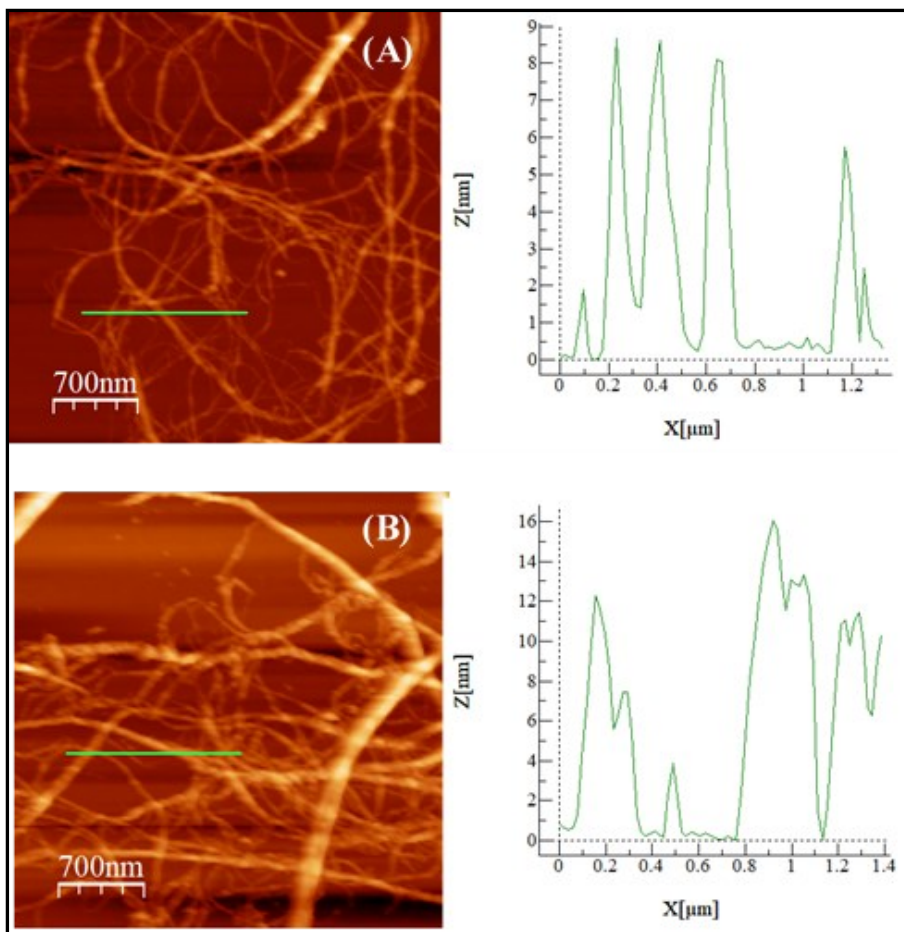


Figure 10. AFM image and corresponding height profile of (A) NFC and (B) NFC-g-PIL

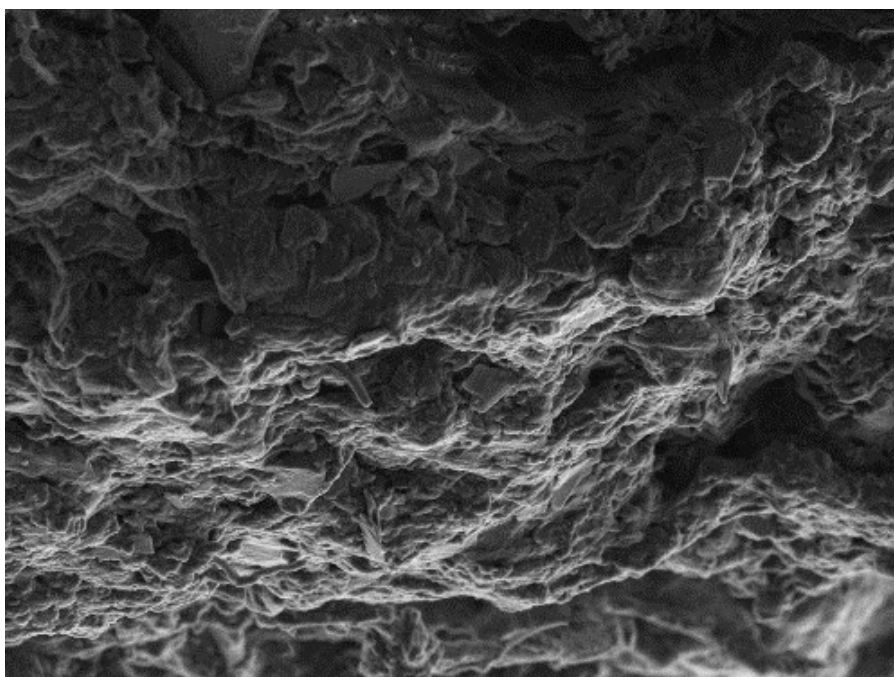


Figure 11. Cross-sectional FESEM image of the rGO1/NFC composite paper